Title	Distinct structural and dynamical difference between supercooled and normal liquids of hydrogen molecules.
Author(s)	Kim, Hyeon-Deuk; Ando, Koji
Citation	Physical chemistry chemical physics : PCCP (2016), 18(4): 2314-2318
Issue Date	2016-01-11
URL	http://hdl.handle.net/2433/207850
Right	This journal is © the Owner Societies 2016; The full-text file will be made open to the public on 11January 2017 in accordance with publisher's 'Terms and Conditions for Self-Archiving'.; This is not the published version. Please cite only the published version. この論文は出版社版でありません。引用の際には出版社版をご確認ご利用ください。
Type	Journal Article
Textversion	author

Distinct Structural and Dynamical Difference between Supercooled and Normal Liquids of Hydrogen Molecules†

Kim Hyeon-Deuk*[a,b] and Koji Ando[a]

Supercooled hydrogen liquid as well as superfluid have continued to elude experimental observation due to rapid crystallization. We computationally realized and investigated supercooled hydrogen liquid by the recently developed non-empirical real-time molecular dynamics method which describes non-spherical hydrogen molecules with the nuclear quantum effects. We demonstrated that the hydrogen supercooled liquid is not a simply cooled liquid but rather exhibits intrinsic structural and dynamical characters including a precursor of tunneling and superfluidity which neither normal hydrogen liquid nor solid possesses. All of the insights provide a milestone for planning experiments of metastable hydrogen systems like glassy and superfluid states and for identifying various unknown hydrogen phases.

1 Introduction

Understanding a supercooled state of liquid is a fundamental open problem in condensed matter physics.[1,2] Knowledge of the mechanisms that govern supercooling of liquids is considered an important step to elucidate not only a nature of glass transitions but also an origin of superfluidity. Particularly for hydrogens, attaining supercooled state as well as superfluid state is still hindered by rapid crystallization in spite of numerous attempts at supercooling liquid hydrogen in macroscopic droplets[3], clusters[4–11], porous media[12,13], or in the bulk[14–16]. One of the most successful approaches is a direct access to the crystallization kinetics of supercooled quantum liquid mixtures of p-H_2 and o-D_2 on submicrosecond time scale recently achieved by Raman spectroscopy of liquid microjets.[15]

Theoretical studies have shown that the inclusion of nuclear quantum effects adds complexity in the behavior of supercooled liquids, leading to novel exotic phenomena such as superfluidity[17,18] or enhanced dynamical slowing down[19,20]. In fact, it has been well established that the thermodynamic and structural properties of the hydrogen liquids and solids as well as their crystallization process are influenced by nuclear quantum effects.[14,15,21–25] Several authors attempted to build a theory of quantum supercooled liquids, but none has so far been able to obtain quantitative results for realistic systems.[17,18]

We recently proposed a simulation method of nuclear and electron wave packet molecular dynamics(NEWPMD) based on non-empirical *ab initio* intra- and inter-molecular interactions of non-spherical hydrogen molecules where important nuclear quantum effects of a hydrogen nucleus were non-perturbatively taken into account.[22,23,26] It reproduced the long-range dispersion interaction depending on an intermolecular angle and can be applied to various phases including normal-pressure liquids and solids. Actually, the NEWPMD gave the correct structures and transport properties such as diffusion coefficients and viscosities of liquid H_2 under vapor pressure without any empirical parameters.[22,23] It also successfully reproduced the stable vapor-pressure solid of the h.c.p. lattice structure with the reasonable freezing temperature and lattice phonon frequencies.[25] The NEWPMD method is thus distinguished from most of the previous semiquantum approaches in which an interaction potential surface was given in advance by a separate modeling with empirical parameters. The non-empirical NEWPMD method enabled the current systematic investigations and quantitative comparisons of the various hydrogen phases.

In this letter, we will report structural and dynamical properties of hydrogen supercooled liquid which are qualitatively different from the hydrogen normal liquid and solid properties. We will demonstrate that the hydrogen supercooled liquid is not just a simply cooled liquid but exhibits new thermodynamic characters including its enhanced quantumness.

2 Computational Method

The NEWPMD approach describes nuclei by floating and breathing Gaussian WPs via the time-dependent Hartree approach, and electron wave packets (EWPs) by the perfect-pairing valence bond theory that appropriately treats the Pauli exclusion energy and intermolecular dispersion energy.[22] The EWP freely changes depending on the H-H bond length $r_{\mathrm{HH}}(t)$; $0.398+0.360r_{\mathrm{HH}}(t)$ Å for the large EWP, and $0.176+0.244r_{\mathrm{HH}}(t)$ Å for the small EWP. These linear dependence of the EWP on $r_{\mathrm{HH}}(t)$ was deduced from the calculation of a H_2 molecule.[26]

[a]*Department of Chemistry, Kyoto University, Kyoto 606-8502, Japan. Fax: +81-75-753-4000; Tel: +81-75-753-4021; E-mail: kim@kuchem.kyoto-u.ac.jp*
[b]*Japan Science and Technology Agency, PRESTO, 4-1-8 Honcho, Kawaguchi, Saitama, 332-0012, Japan*

† Electronic Supplementary Information (ESI) available: Additional structural and dynamical information on supercooled hydrogen molecules.

The supercooled liquid systems were composed of 640 H_2 molecules in a cubic simulation box with a periodic boundary condition. All the intermolecular interaction forces decay to zero in the 5 % edge of the box length. Density of the supercooled hydrogen liquid was set by extrapolating the saturated vapor-pressure line toward the lower temperature region[27]; *e.g.* the molar volume is $24.2 \times 10^{-6}\mathrm{m}^3/\mathrm{mol}$ at 2.5 K, $24.4 \times 10^{-6}\mathrm{m}^3/\mathrm{mol}$ at 5 K, $25.1 \times 10^{-6}\mathrm{m}^3/\mathrm{mol}$ at 10 K, $25.5 \times 10^{-6}\mathrm{m}^3/\mathrm{mol}$ at 12 K, and $25.8 \times 10^{-6}\mathrm{m}^3/\mathrm{mol}$ at 13 K which are all larger than the solid molar volume[25]. We started cooling and equilibration runs from the h.c.p. crystal structure where each hydrogen molecule has random orientation. We made the atomic center momentum degrees of freedom influenced by the heat bath set by the velocity scaling thermostat and Berendsen methods for hundreds of picoseconds at each temperature. All integrations of the equations of motion were performed by the velocity-verlet method with the time step 0.1 fs for the cooling and equilibration runs. After the equilibration runs, we carried out the NVE (microcanonical) simulations for hundreds of picoseconds with the time step 0.5 fs. The computational costs for the NEWPMD were reasonable; propagating 640 molecules including H-H bond vibrations and NWP breathings for 1 ps required only 18 minutes on a single core of a Xeon CPU with 2.67 GHz.

3 Results and Discussions

3.1 Basic properties of supercooled hydrogen liquids

Figure 1(a) shows radial distribution functions (RDFs) of supercooled liquid and solid at 2.5 K. The RDF of the supercooled liquid has no long-range periodic structure unlike the solid RDF. The split double-peak in 3.0-4.2 Å is shifted toward the shorter distance in the supercooled liquid than in the solid in spite of the lower overall density in the former. This comes from the qualitative structural difference; the supercooled liquid has the rigid T-shape structure in the first solvation shell, while the solid maintains the zigzag lattice configuration to realize the long-range stable lattice.[25] We note that integration up to the minimum at 4.8 Å of the supercooled liquid gave a lower value than the solid peak integration reflecting its lower density. The first peak at 3.1 Å less intense than the second peak at 3.8 Å also indicates freer orientational motions in the supercooled liquid and thus its liquidity even at 2.5 K. As shown in Fig.S1†, however, the main peak position and its width did not shift nor change at 2.5 K through 13 K due to stiffness of the first solvation shell of the supercooled liquid; only the relative intensity of the first peak over the second peak decreased with increasing the temperature reflecting freer orientational motions at the higher temperature.

A mean square displacement (MSD) effectively characterizes phase- and timescale-dependent dynamics and thus has been used as one of the important factors to analyze supercooled and glassy phases.[28,29] The MSD of the supercooled liquid at 2.5 K shown in Fig.1(b) exhibited a few characteristic stages and was not on a simple line. The initial increase of the MSD up to 0.15 $\mathrm{Å}^2$ corresponds to phonon motions inside a mesoscale lattice cluster which persistently remains in the supercooled liquid at 2.5 K and may be called local-β relaxation.[30–32] The following phonon-plateau stage continued for a long time, approximately 100 ps, indicating quasi-solidification of the supercooled liquid. However, the metastable H_2 clusters slowly deformed as appearing in the slow increase of the MSD after 100 ps which corresponds to α-relaxation.[30–32] This slow-collapse stage of the phonon modes in the lattice cluster does not necessarily indicate a cage breakout but rather mesoscale lattice deformation as will be discussed in Fig.3. As shown in Fig.S1†, transitions of these stages happened in shorter interval and the phonon-plateau stage almost diminished with increasing the temperature.

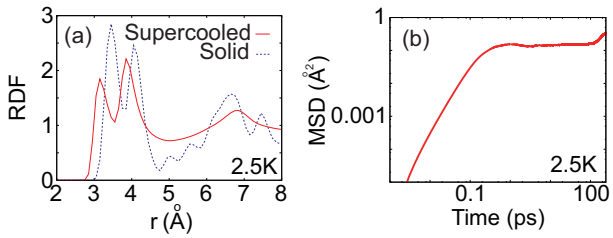

Fig. 1 (a) Comparison of RDFs of the supercooled liquid and solid at 2.5 K. The RDF of the supercooled liquid did not have a long-range periodic structure and its first peak appeared at the shorter distance in spite of the lower overall density. (b) MSD of the supercooled liquid at 2.5 K. The MSD showed plateau and collapse stages and was not on a linear line.

3.2 Boson peaks originated from partially broken lattice phonon modes

Figure 2 displays power spectra for a real-time coordinate displacement of each hydrogen atom in the space-fixed frame. We found that the current H_2 supercooled liquid exhibits the broad low-frequency peaks which can be assigned as a boson peak analogous to those observed in various glasses and supercooled liquids.[28,29,33–35] The boson peak frequency redshifted and the peak intensity grew with increasing the temperature as shown in Fig.S8†. The redshifting peaks are qualitatively different from the constant peaks of the lattice phonon observed in the H_2 solid.[25,36] This boson peak almost disappeared above the melting temperature of 14 K, indicating that molecular dynamics causing the boson peak is closely related to metastability. The frequency of the boson peak at the lower temperature continuously approaches the frequency

of the lattice phonon mode in the H_2 solid, 40 cm^{-1}.[25] This continuous frequency redshift from the solid phonon peak to the supercooled liquid boson peak demonstrates that the current boson peak stemmed from partially broken phonon modes in a metastable lattice cluster. Actually, the metastable phonon modes and their slow collapse were seen in the MSD of Fig.1(b). As discussed there, the formation and collapse of the metastable lattice clusters highly depend on the temperature; the redshifts of the boson peak can be explained by the fact that the metastable lattice clusters become more fragile at the higher temperature. Note that the NEWPMD involves no empirical parameter and thus the present systematic analysis from the solid to the supercooled liquid is free from any parameter refitting depending on the temperature and phases. There was another peak around 5 cm^{-1} which we attributed to translational dynamics of H_2 molecules related to the MSDs in Fig.1(b) and Fig.S1; the peak became enhanced with increasing the temperature up to the normal liquid region while it disappeared at the lower temperature where the significant translational motions were almost frozen.(See Fig.S3†) All of these properties as well as the lower peak frequency region are different from the properties which the above boson peak has. The frozen translational dynamics was also supported by the Gaussian decays of the time correlation functions of the angular dynamics at the extremely lower temperature shown in Figs.S4, S5 and S7†; a hydrogen molecule confined in a stable lattice can change its orientation more freely, leading to the faster inertial Gaussian decay.

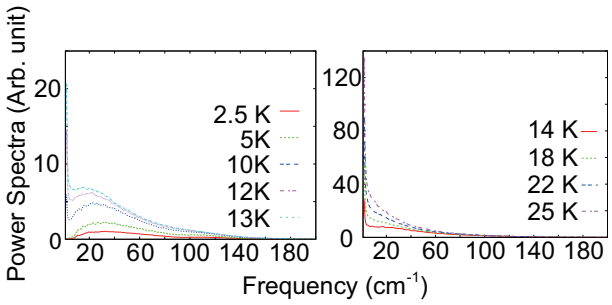

Fig. 2 Low-frequency power spectra of the space-fixed coordinate displacement of the supercooled and normal liquids. Boson peaks appeared only in the supercooled liquid states. The current boson peak stemmed from partially broken phonon modes in a metastable lattice cluster. Peaks around 5 cm^{-1} reflected translational motions of H_2 molecules and disappeared at the extremely lower temperature.

3.3 Difference between diffusive dynamics of supercooled and normal hydrogen liquids

Figure 3(a) shows correlation times of the angular dynamics in the supercooled liquid deduced from Figs.S4, S5 and S7†. These long-time angular dynamics are closely related to diffusive dynamics of H_2 molecules.[23]. We found that the correlation times were not on a universal exponential function but on the two different exponential functions, $\exp(-T/3)$ for the supercooled liquid region below 13 K and $\exp(-T/6)$ for the liquid region above 14 K, indicating that the supercooled liquid and normal liquid of H_2 have different intrinsic dynamics of diffusion. The MSDs of Fig.1 and Fig.S1† suggest that the diffusive dynamics involving large configurational rearrangements such as cage breakout became drastically suppressed in the supercooled liquid below 13 K and that mesoscale cluster deformations started to dominate the diffusive dynamics. As a result, the kinetic timescales in and out of a cluster became well separated as shown by the step-wise MSD. This suggestion was also supported by the fact that the difference between the long correlation times of the intermolecular angle θ and the self-orientations ϕ and ω was more enhanced with increasing the temperature; the diffusion out of a cluster at the higher temperature induced the faster correlation decay of the intermolecular angle θ which is more sensitive to the diffusive dynamics. In addition, as shown in Fig.S9†, the short correlation times, which correspond to kinetic dynamics inside a cluster, were on the single linear line regardless of the temperature; the non-diffusive dynamics did not qualitatively change depending on the phases. If the diffusion below 13 K was still caused by a cage breakout as in the normal liquid case, we should observe the similar non-uniform temperature dependence even in the short-time dynamics. The current distinct difference between the dynamics of the supercooled liquid and normal liquid was similarly found in the librational frequency (Fig.S9†), in the average H-H bond length as well as its vibrational frequency (Fig.S10†) and in the nuclear wave packet(NWP) beating frequency (Fig.S11†). It should be noted that the H-H vibrational frequency for the supercooled liquid shown in Fig.S10† agrees well with the previous experimental observation that the vibrational frequency of the liquid p-H_2 clusters is higher than that in solid, but lower than that in the bulk liquid.[16]

We further rationalized the distinctive change of the correlation times by introducing the structural order parameter in Fig.3(b). The order parameter was defined by an integration of the first peak of the RDF at each temperature. These order parameters directly reflect stiffness of a T-shape coordination formed by nearest-surrounding H_2 molecules and thus can be a structural order parameter to represent formations and deformations of a mesoscale cluster. We again found that the order parameters were not on a universal line but on the two different linear functions, indicating that the distinctive change in the formation and deformation of nearest-surrounding molecules happened at the melting point. As reported in Fig.S9†, temperature-dependent librational frequencies also exhibited the significant change at the melting point

and can be used to monitor various phases including the supercooled liquid.[15] The acceleration of the diffusive dynamics above 14 K is closely linked to melting above 14 K and clearly distinguishes the normal liquid from the supercooled liquid.[16]

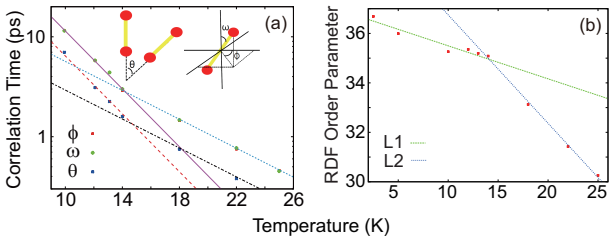

Fig. 3 (a) Correlation times of the intermolecular angle θ and the self-orientations ϕ and ω. The correlation times were fitted by the two different exponential functions. $\exp(-T/3)$ for the supercooled liquid and $\exp(-T/6)$ for the normal liquid originated from the different diffusive dynamics, mesoscale cluster deformations and cage breakouts, respectively. (b) Structural order parameters calculated by an integration of the first peak of the RDF. The order parameters on the two different linear functions, L1=-0.133x+36.8 and L2=-0.439x+41.1, indicated the distinctive change in the formation and deformation of nearest-surrounding H_2 molecules below and above the melting point.

3.4 Enhanced quantumness in supercooled hydrogen liquid

Figure 4(a) shows extent of nuclear delocalization as distributions of the NWP width. The distributions became sharper as the temperature decreased from 22 K down to 10 K corresponding to shrinking of the distributions of the H-H bond length shown in Fig.S10†. However, the distributions of the NWP width at below 10 K were similar or even broader compared to the 10 K distribution, which cannot be explained by the suppressed thermal fluctuations of the H-H bond length at the extremely low temperature.

Figure 4(b) rationalizes this seemingly inconsistent tendency by introducing a measure of quantumness. We defined the quantumness by a ratio of peak height of the r_{HH}-distribution over peak height of the NWP width distribution given in Fig.S10† and Fig.4(a), respectively. The NWP width is related to the H-H bond length which is mainly determined by the thermal fluctuation as in Fig.S10†; as the H-H length increases, the NWP becomes more delocalized, and *vice versa*. This is why we introduced the quantumness by the ratio of peak height of the r_{HH}-distribution over peak height of the NWP width distribution. Actually, the defined quantumness can measure extent of nuclear delocalization which is not simply correlated to the bond length r_{HH}; the quantumness should be constant as far as the nuclear delocalization is purely linked to the r_{HH} fluctuation as the cases above 10 K showed in the figure. Since the defined quantity measured extent of nuclear delocalization which is a typical nuclear quantum effect, we called this quantity quantumness. Figure 4(b) demonstrates that the quantumness became extremely enhanced at below 10 K in the supercooled liquid than in the solid or in the normal liquid. The rapid growth of the quantumness can be explained by the frozen translational motion at the extremely low temperature, as evidenced by the disappearance of the translational peak in Fig.2, by the disappearance of H_2 molecules of high kinetic energy in Fig.S3† and by the ordered orientational distributions in Fig.S4†. On one hand, at the extremely low temperature, the NWP was more delocalized in the stable and rigid cluster with little translational dynamics; a NWP is attracted from electron wave packets located at the center of nearest-surrounding H_2 molecules. On the other hand, NWPs of H_2 molecules out of a cluster kept shrunk since the cluster formation is hindered in the low temperature due to the little translational energy. These two contrasting facts rationalize the broadened distributions of the NWPs at the extremely low temperature. The closer T-shape configuration of the supercooled liquid than the zigzag configuration of the solid, as shown in Fig.1(a), also let NWPs more influenced by surrounding H_2 molecules and thus contributed to the enhanced quantumness compared to the solid case. In these senses, the current anomalous quantumness is intrinsic to the supercooled liquid. The delocalization of the NWP at the extremely low temperature, which has little correlation with the H-H bond length, should be a precursor of tunneling and superfluidity of H_2 molecules. Such strong nuclear quantum phenomena will finally occur at further lower temperature of approximately 1 K.[15]

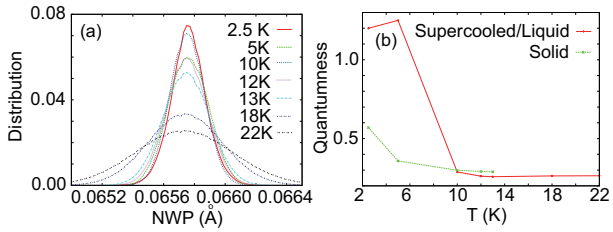

Fig. 4 (a) Distributions of the NWP width. The distributions simply reflected thermal fluctuations from 22 K to 10 K, while the distributions at below 10 K were similar or even broader compared to the 10 K case. (b) Quantumness defined by a ratio of peak height of the r_{HH}-distribution over peak height of the NWP width distribution. The quantumness was more enhanced at below 10 K in the supercooled liquid than in the solid or in the normal liquid.

4 Concluding Remarks

In summary, we computationally demonstrated that the supercooled hydrogen liquid exhibits distinct structural and dynamical properties such as closer first peak of the RDF than the solid RDF, non-linear MSD, red-shifting boson peaks with increasing temperature, diffusion caused by mesoscale cluster deformation, and enhanced localization and delocalization of hydrogen nuclei. We concluded that these properties are intrinsic to the supercooled liquid since they were never obtained in the normal hydrogen liquid and solid. All of the insights and information we obtained in this paper will help in planning experiments focusing on hydrogen metastable states and in rationalizing the experimental data. Especially, monitoring the low-frequency modes below 100 cm^{-1} as well as frequencies of the angular dynamics will play a pivotal role in identifying and characterizing unknown thermodynamic states. Superfluidity, which is predicted to appear at around 1 K, will be examined in a forthcoming paper by accounting for nuclear exchange effects in the current NEWPMD method.

5 Acknowledgments

KHD thanks the financial supports from JST (PRESTO), and Grant-in-Aids for Scientific Research from Japan Society for the Promotion of Science (KAKENHI), Grant No. 24750016. KA acknowledges support from KAKENHI No. 22550012 and 26620007.

References

1 S. Tatsumi, S. Aso and O. Yamamuro, *Phys. Rev. Lett.*, 2012, **109**, 045701.
2 M. D. Ediger and P. Harrowell, *J. Chem. Phys.*, 2012, **137**, 080901.
3 H. J. Maris, G. M. Seidel and F. I. B. Williams, *Phys. Rev. B*, 1987, **36**, 6799.
4 G. Tejeda, J. M. Fernandez, S. Montero, D. Blume and J. P. Toennies, *Phys. Rev. Lett.*, 2004, **92**, 223401.
5 H. Li, R. J. Le Roy, P.-N. Roy and A. R. W. McKellar, *Phys. Rev. Lett.*, 2010, **105**, 133401.
6 Y. Kwon and K. B. Whaley, *Phys. Rev. Lett.*, 2002, **89**, 273401.
7 S. A. Khairallah, M. B. Sevryuk, D. M. Ceperley and J. P. Toennies, *Phys. Rev. Lett.*, 2007, **98**, 183401.
8 P. Sindzingre, D. M. Ceperley and M. L. Klein, *Phys. Rev. Lett.*, 1991, **67**, 1871.
9 K. Kuyanov-Prozument and A. F. Vilesov, *Phys. Rev. Lett.*, 2008, **101**, prl205301.
10 T. Zeng and P.-N. Roy, *Rep. Prog. Phys.*, 2014, **77**, 046601.
11 S. Grebenev, B. Sartakov, J. P. Toennies and A. F. Vilesov, *Science*, 2000, **289**, 1532.
12 J. D. Kinder, A. Bouwen and D. Schoemaker, *Phys. Rev. B*, 1995, **52**, 15872.
13 M. Schindler, A. Dertinger, Y. Kondo and F. Pobell, *Phys. Rev. B*, 1996, **53**, 11451.
14 M. Kuhnel, J. M. Fernandez, G. Tejeda, A. Kalinin, S. Montero and R. E. Grisenti, *Phys. Rev. Lett.*, 2011, **106**, 245301.
15 M. Kuhnel, J. M. Fernandez, F. Tramonto, G. Tejeda, E. Moreno, A. Kalinin, M. Nava, D. E. Galli, S. Montero and R. E. Grisenti, *Phys. Rev. B*, 2014, **89**, 180201.
16 R. Sliter and A. F. Vilesov, *J. Chem. Phys.*, 2009, **131**, 074502.
17 F. Zamponi, *Nat. Phys.*, 2011, **7**, 99.
18 O. N. Osychenko, R. Rota and J. Boronat, *Phys. Rev. B*, 2012, **85**, 224513.
19 T. E. Markland, J. A. Morrone, B. J. Berne, K. Miyazaki, E. Rabani and D. R. Reichman, *Nat. Phys.*, 2011, **7**, 134.
20 T. E. Markland, J. A. Morrone, K. Miyazaki, B. J. Berne, D. R. Reichman and E. Rabani, *J. Chem. Phys.*, 2012, **136**, 074511.
21 M. Zoppi, *J. Phys. Cond. Mett.*, 2003, **15**, R1047.
22 K. Hyeon-Deuk and K. Ando, *J. Chem. Phys.(Communication)*, 2014, **140**, 171101.
23 K. Hyeon-Deuk and K. Ando, *Phys. Rev. B*, 2014, **90**, 165132.
24 H. Saito, H. Nagao, K. Nishikawa and K. Kinugawa, *J. Chem. Phys.*, 2003, **119**, 953.
25 K. Hyeon-Deuk and K. Ando, *J. Chem. Phys.(Communication)*, 2015, **140**, 171102.
26 K. Hyeon-Deuk and K. Ando, *Chem. Phys. Lett.*, 2012, **532**, 124.
27 Y. Yonetani and K. Kinugawa, *J. Chem. Phys.*, 2004, **120**, 10624.
28 J. Helfferich, F. Ziebert, S. Frey, H. Meyer, J. Farago, A. Blumen and J. Baschnagel, *Phys. Rev. E*, 2014, **89**, 042603.
29 J. Helfferich, F. Ziebert, S. Frey, H. Meyer, J. Farago, A. Blumen and J. Baschnagel, *Phys. Rev. E*, 2014, **89**, 042604.
30 H. Vogel, *Phys. Z.*, 1921, **22**, 645.
31 G. S. Fulcher, *J. Am. Ceram. Soc.*, 1923, **8**, 339.
32 K. L. Ngai and M. Paluch, *J. Chem. Phys.*, 2004, **120**, 857.
33 O. Yamamuro, I. Tsukushi, T. Kanaya and T. Matsuo, *J. Phys. Chem. Sol.*, 1999, **60**, 1537.
34 O. Yamamuro, K. Takeda, I. Tsukushi and T. Matsuo, *Physica B*, 2002, **311**, 84.
35 O. Yamamuro, Y. Madokoro, H. Yamasaki, T. Matsuo, I. Tsukushi and K. Takeda, *J. Chem. Phys.*, 2001, **115**,

9808.
36 S. Ciliberti, T. Grigera, V. Martin-Mayor, G. Parisi and P. Verrocchio, *arXiv:cond-mat/0312073*, 2003.

Distinctive Structural and Dynamical Difference between Supercooled and Normal Liquids of Hydrogen Molecules

Kim Hyeon-Deuk[1,2,*] and Koji Ando[1]

[1]Department of Chemistry, Kyoto University, Kyoto, 606-8502, Japan

[2]Japan Science and Technology Agency, PRESTO, 4-1-8 Honcho, Kawaguchi, Saitama, 332-0012, Japan

[*]Corresponding author: kim@kuchem.kyoto-u.ac.jp

Supporting Figures

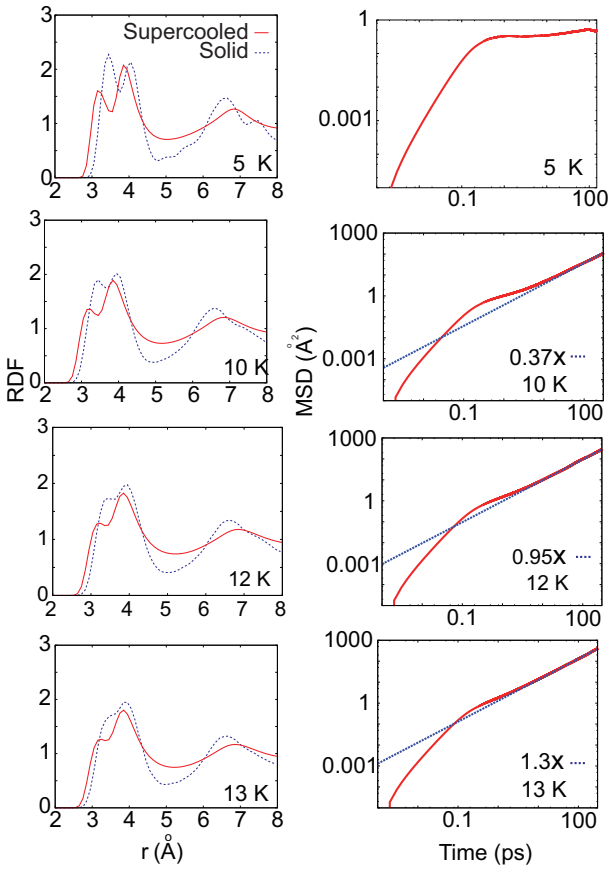

Figure S1: Radial distribution functions (RDFs) and mean square displacements (MSDs) of the supercooled liquid at the other temperature. The first peak of the supercooled liquid RDF was lower than the second peak and the first peak was closer than the corresponding peak of the solid RDF at all the temperatures. The first peak position and its width did not shift nor change at 2.5 K through 13 K being in harmony with the normal liquid RDF.[1, 2] The relative intensity of the first peak over the second peak is determined by thermal modulations of H2 molecules in the

first solvation shell including the translational and orientational motions. In fact, the relative intensity decreased with increasing the temperature. The corresponding two-dimensional (2D) RDFs are given in Fig.S2. The MSDs of the supercooled liquid were nonlinear unlike the linear MSD of the normal liquid and had the plateau- and collapse-stages. Transitions of each stage happened more shortly and the plateau stage became harder to identify with increasing the temperature.

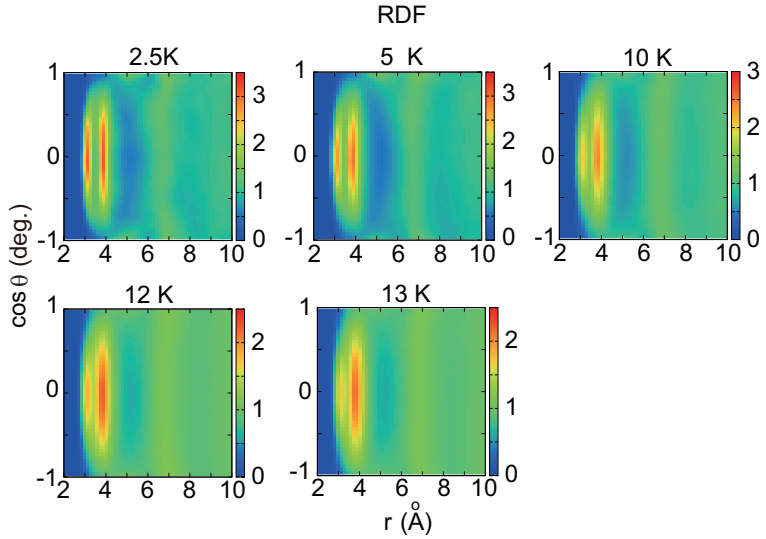

Figure S2: 2D RDFs as a function of a radial coordinate r and the intermolecular angle θ.[2] No long-range periodic structure was obtained unlike the 2D RDFs of the H_2 solid. The whole shapes were rather close to the 2D RDFs of the normal liquid.[2, 3]

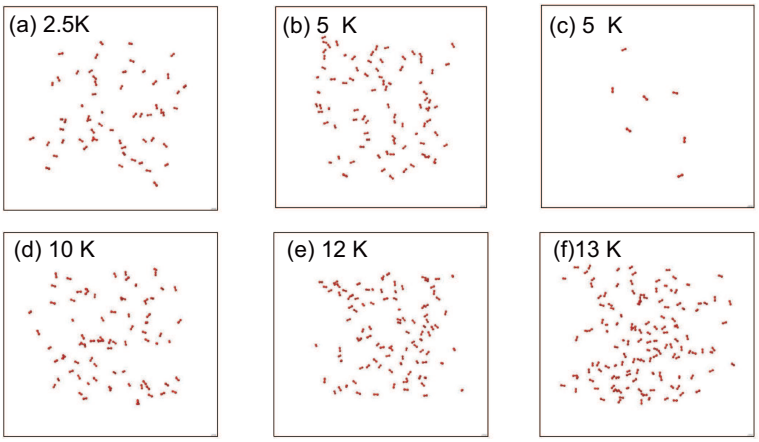

Figure S3: Snap shots of H_2 molecules which have kinetic energy larger than (a) 3.00 K, (b) 5.89 K, and (c-f) 12.0 K. As seen in (a), (b) and (d-f), H_2 molecules of high kinetic energy did not exist randomly but rather irregularly in the simulation box, which is a typical property of supercooled liquid. The panel (c) demonstrates that there were only a few H_2 molecules having kinetic energy higher than 12.0 K and significant translational motions were almost frozen at the temperature of 5 K. This fact rationalizes the disappearance of the translational peak at the extremely lower temperature in Fig.2.

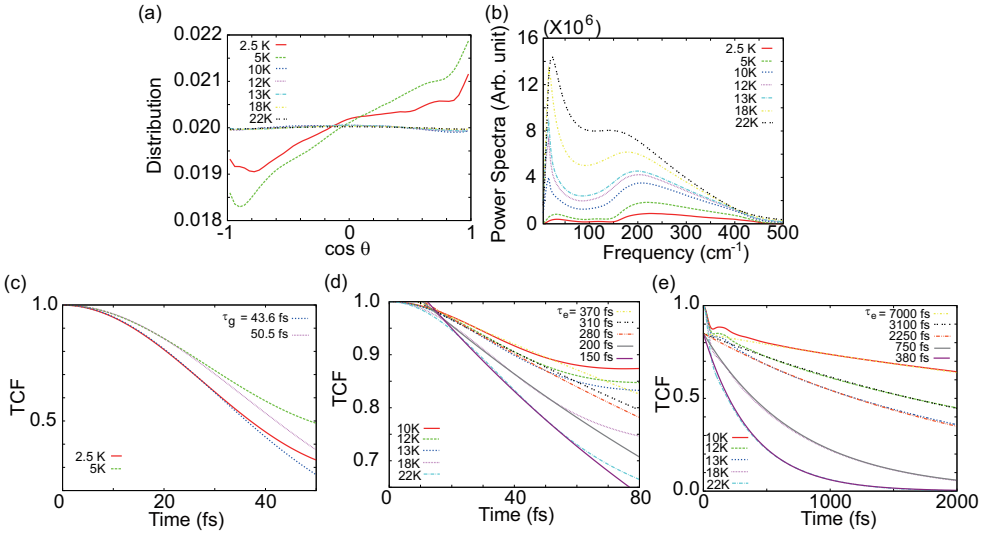

Figure S4: (a) Distributions of the intermolecular angle $\cos\theta$ in the supercooled liquid. The distribution was almost uniform at above 10 K, while it became ordered at the extremely low temperature due to the frozen translational dynamics at below 10 K. The distribution at 5 K was more ordered than the distribution at 2.5 K because the lattice clusters were formed more stably at 2.5 K and the H_2 molecules could change their orientation more freely; partially broken lattice clusters have more orientationally ordered structures in the supercooled liquid. We note that, however, the difference in the distributions at 2.5 K and 5 K is quite small and the relative intensity of the first RDF peak over the second RDF peak in Fig.1(a) and Fig. S1 is determined by total thermal modulations of H_2 molecules including the translational and orientational motions. Actually, the orientational distribution at 5 K is much more uniform than the periodic orientational distributions of the hydrogen solid at any temperature.[3] (b) Power spectra of the intermolecular angle θ in the supercooled liquid obtained by a Fourier transformation of time-dependent $\theta(t)$. The librational peak around 200 cm^{-1} redshifted with increasing the temperature reflecting the softened librational potential in a more broken T-shape solvation structure. Relatively stable clusters at below 10 K enabled mixing of the phonon and orientational dynamics inside a cage, leading to the boson peaks around 25 cm^{-1} even in the θ-power spectra. (c-e) Time correlation functions of $\theta(t)$ in the supercooled H_2 liquid. The Gaussian decay appeared at the extremely low temperature due to formation of the relatively stable lattice clusters. The estimated timescale at 2.5 K was shorter than the timescale at 5 K reflecting the more stable lattice cluster at 2.5 K where H_2 molecules can change their orientation more freely. In the exponential decay at above 10 K, the estimated decay timescales simply decreased with increasing the temperature purely reflecting the faster thermal kinetic motions at the higher temperature.

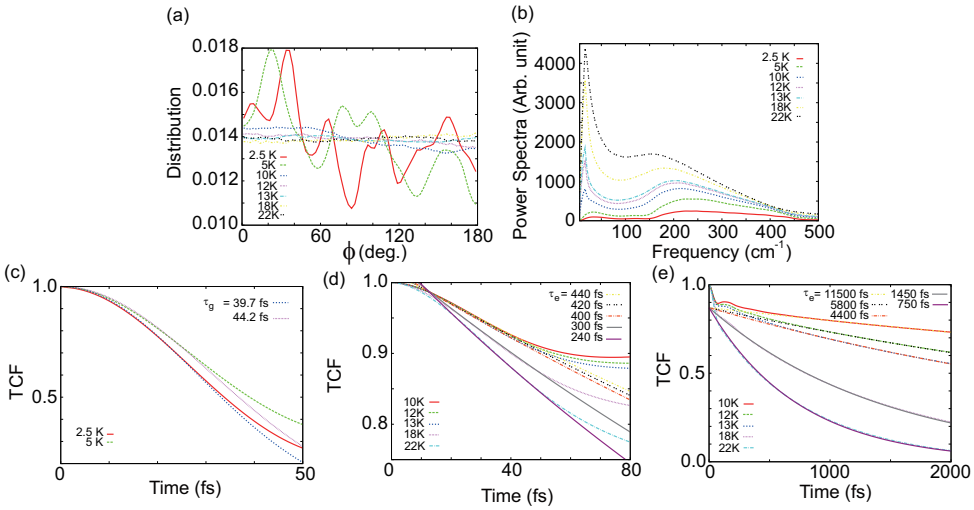

Figure S5: Same as Fig.S4, but for the self-orientation ϕ. The difference between the distributions at 2.5 K and 5 K was smaller compared to the case of the intermolecular angle θ. This is because the self-orientations were less influenced by the stable formation of the lattice cluster than the intermolecular angle. The two-dimensional(2D) distributions of the self-orientations ϕ and ω are given in Fig.S6.

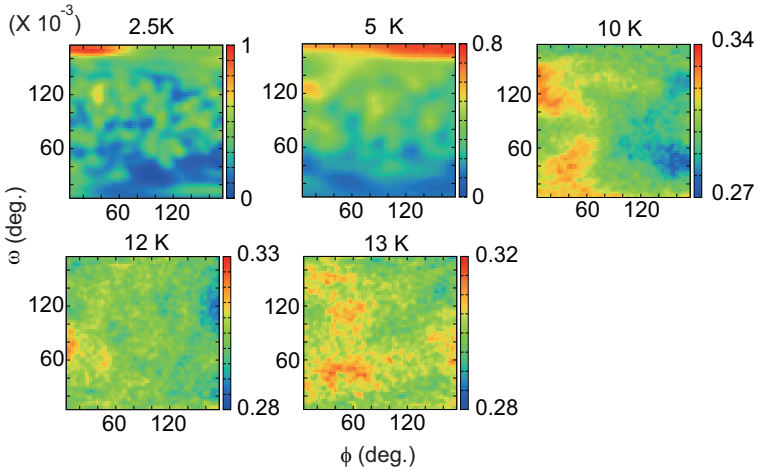

Figure S6: 2D distributions of the self-orientations ϕ and ω in the supercooled liquid. The distributions were almost uniform at above 10 K, while the distributions at below 10 K were slightly ordered. Mesoscale lattice clusters persistently remained due to the frozen translational motions at the extremely low temperature, resulting in the ordered orientations.

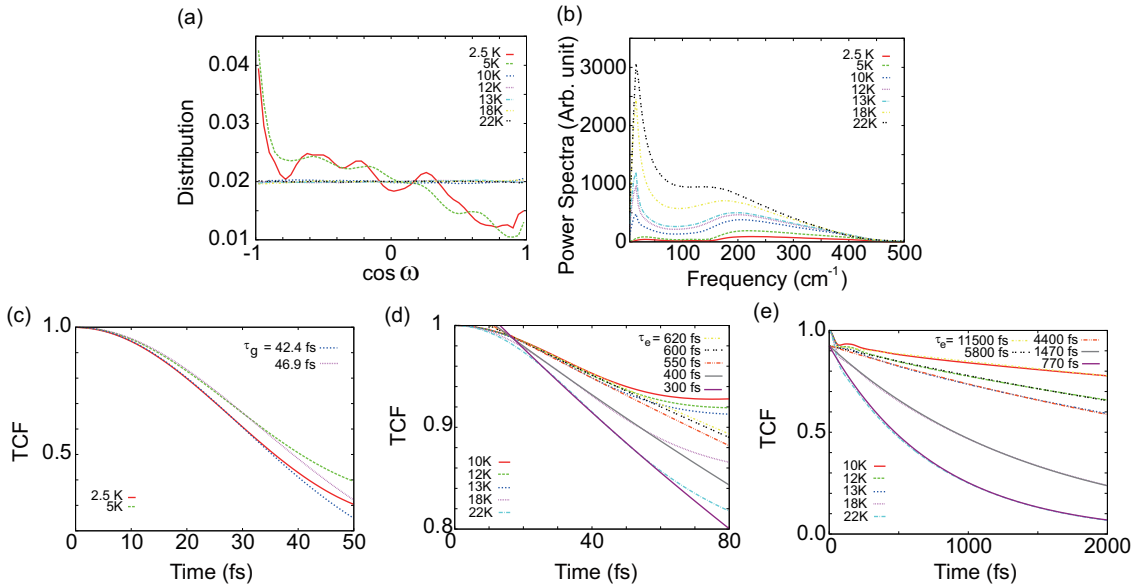

Figure S7: Same as Fig.S5, but for the self-orientation ω.

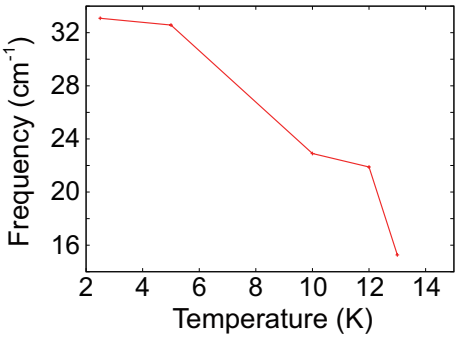

Figure S8: Boson peak frequencies deduced from Fig.2. Note that the boson peak almost disappeared above the melting temperature.

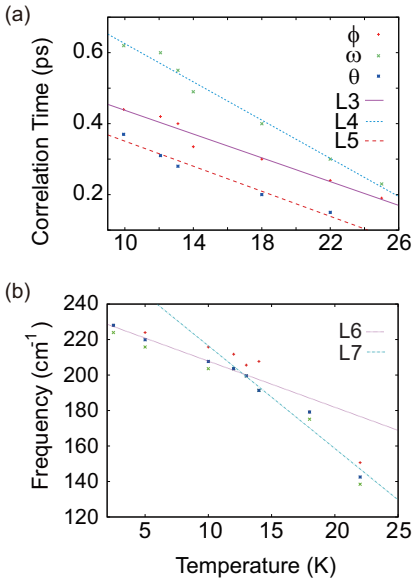

Figure S9: (a) Short correlation times of the self-orientations ϕ and ω and the intermolecular angle θ as a function of temperature. The short correlation times simply reflect kinetic dynamics inside a cluster and were on the single linear line: L3=$16.75x + 605.2$, L4=$-26.93x + 894.7$, and L5=$-17.65x + 527.2$. We note that the decay of the correlation function at below 10 K was reproduced only by the single Gaussian function not by the multiple exponential functions. This is because the translational motions such as cluster deformations were almost suppressed at below 10 K, and the correlations were decayed by the simple orientational motions inside a lattice cluster.

(b) Librational frequencies as a function of temperature. The frequencies were deduced from the peak frequencies of the corresponding angular power spectra in Figs.S4, S5, and S7. The librational frequency redshifted with increasing the temperature since the librational potential became softer with the more broken neighboring structure. All the librational frequencies were fitted by the two lines not by a universal line: L6=$-2.600x$+233.8 and L7=$-5.790x$+274.4. The origin of the distinctive difference between the librational dynamics of the supercooled liquid and the normal liquid was discussed from the view point of the structural order parameter in Fig.3. This panel suggests that observing librational frequency can monitor various phases including the supercooled liquid. Especially, the supercooled liquid phase can be distinguished from the normal liquid phase by observing the temperature dependence of the librational frequency as well as the H-H vibrational frequency shown in Fig.S10.[4, 5]

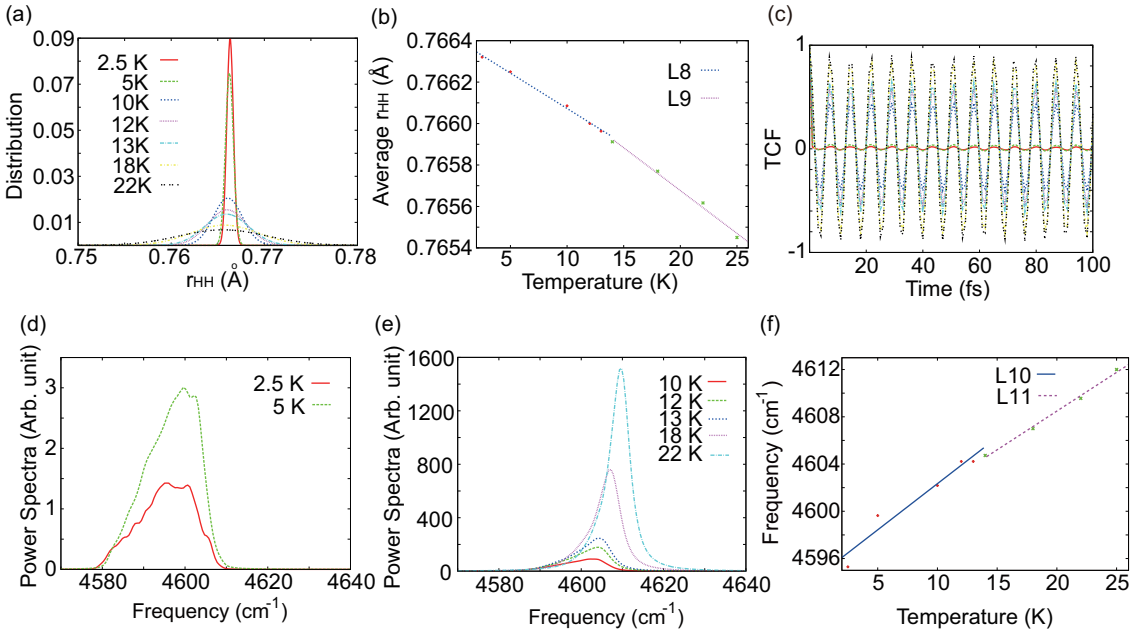

Figure S10: (a) Distributions of the H-H bond length r_{HH}. The r_{HH}-distributions at the lower temperature were sharper than the r_{HH}-distributions of the H_2 solids since the T-shape solvation coordinate in the supercooled liquid was much simpler than the zigzag asymmetric structures in the solids.[3] The r_{HH}-distributions of the supercooled liquid at the higher temperature were rather broader than the r_{HH}-distributions of the H_2 solids simply reflecting the larger thermal modulations by the significant translational motions.

(b) Averages of the H-H bond length r_{HH} as a function of temperature. The average r_{HH} linearly decreased with increasing the temperature due to the more broken T-shape structure at the higher temperature.[2] The average r_{HH} was fitted by the two lines not by a universal line: L8$=-3.410\times10^{-5}x+0.7664$ for below 13 K and L9$=-4.130\times10^{-5}x+0.7665$ for above 14 K. The origin of the distinctive difference between the supercooled liquid and the normal liquid was discussed in Fig.3.

(c) Time correlation functions of the H-H bond length r_{HH} as a function of time. The amplitude was linked to the width of the r_{HH}-distributions.

(d and e) Power spectra of the time-dependent H-H bond length $r_{HH}(t)$. The power spectra at 2.5 K and 5 K had the complicated multiple peaks which stemmed from the metastable lattice clusters remaining in the supercooled liquid. The peak height was simply proportional to the temperature in contrast with the nuclear wave packet(NWP) case discussed in Fig.4.

(f) The H-H vibrational frequency as a function of temperature deduced from the peak positions of the above power spectra. The H-H frequency linearly increased with increasing the temperature but was fitted by the two lines not by

a universal line: L10=$0.7818x + 4595$ for below 13 K and L11=$0.6556x + 4595$ for above 14 K. The blue shifting H-H vibrational frequency is attributed to the shrinking H-H bond length.

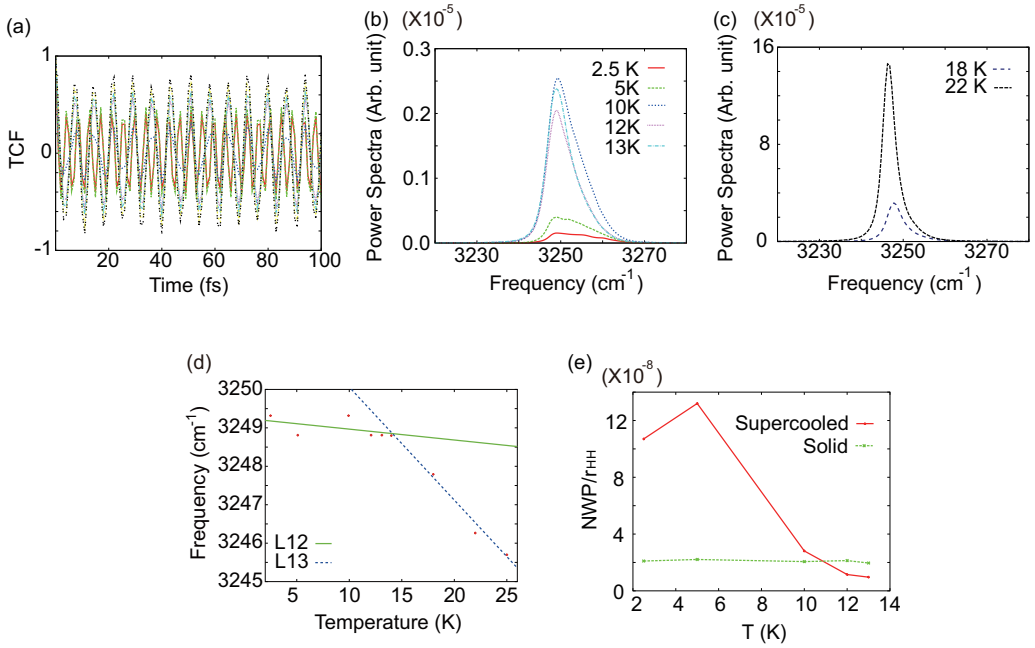

Figure S11: (a) Time correlation functions of the NWP width as a function of time. The amplitude is linked to the variations of the NWP width-distributions in Fig.4(a).

(b and c) Power spectra of the time-dependent NWP width. The power spectra at the lower temperature had complicated multiple peaks which stemmed from the metastable lattice clusters remaining in the supercooled liquid. The peak height was not simply proportional to the temperature as discussed in Fig.4.

(d) The NWP beating frequency as a function of temperature deduced from the peak positions of the above power spectra. The beating frequency linearly decreased with increasing the temperature but was fitted by the two lines not by a universal line: L12=$-0.02830x + 3249$ for below 13 K and L13=$-0.2940x + 3253$ for above 14 K. This is simply attributed to the structural order parameter shown in Fig.3; the delocalized NWP width as well as the elongated H-H bond in the rigid T-shape structure at the lower temperature made the NWP beating potential more isolated and sharper.

(e) Another quantumness defined by a ratio of the peak height of the NWP power spectra over the peak height of the r_{HH}-power spectra given in Fig.S11 and Fig.S10, respectively. The defined quantumness can measure extent of thermal modulations of the NWP beating compared to the H-H vibrations. This quantumness should be constant as

far as the NWP beating is purely linked to the r_{HH} vibrations as in the shown solid case. The current quantumness became enhanced at below 10 K in the H_2 supercooled liquid in harmony with the original quantumness discussed in Fig.4.

---

[1] K. Hyeon-Deuk and K. Ando, J. Chem. Phys.(Communication) **140**, 171101 (2014).

[2] K. Hyeon-Deuk and K. Ando, Phys. Rev. B **90**, 165132 (2014).

[3] K. Hyeon-Deuk and K. Ando, J. Chem. Phys.(Communication) **140**, 171102 (2015).

[4] M. Kuhnel, J. M. Fernandez, F. Tramonto, G. Tejeda, E. Moreno, A. Kalinin, M. Nava, D. E. Galli, S. Montero, and R. E. Grisenti, Phys. Rev. B **89**, 180201 (2014).

[5] G. Geneste, M. Torrent, F. Bottin, and P. Loubeyre, Phys. Rev. Lett. **109**, 155303 (2012).